THE JOURNAL OF BIOLOGICAL CHEMISTRY VOL. 283, NO. 26, pp. 18076–18085, June 27, 2008

N-type Inactivation of the Potassium Channel *KcsA* by the *Shaker* B "Ball" Peptide

*MAPPING THE INACTIVATING PEPTIDE-BINDING EPITOPE**

Received for publication, December 12, 2007, and in revised form, April 7, 2008 Published, JBC Papers in Press, April 22, 2008, DOI 10.1074/jbc.M710132200

M. Luisa Molina[‡1,2], Francisco N. Barrera[‡1,3], José A. Encinar[‡], M. Lourdes Renart[‡2], Asia M. Fernández[‡], José A. Poveda[‡], Jorge Santoro[§], Marta Bruix[§], Francisco Gavilanes[¶], Gregorio Fernández-Ballester[‡], José L. Neira[‡‖], and José M. González-Ros[‡4]

From the [‡]Instituto de Biología Molecular y Celular, Universidad Miguel Hernández, 03202 Elche (Alicante) , the [§]Instituto de Química-Física Rocasolano, CSIC, 28006 Madrid, the [¶]Departamento de Bioquímica, Facultad de Ciencias Químicas, Universidad Complutense, 28040 Madrid, and the [‖]Biocomputation and Complex Systems Physics Institute, 50009 Zaragoza, Spain

The effects of the inactivating peptide from the eukaryotic *Shaker* B K^+ channel (the ShB peptide) on the prokaryotic KcsA channel have been studied using patch clamp methods. The data show that the peptide induces rapid, N-type inactivation in KcsA through a process that includes functional uncoupling of channel gating. We have also employed saturation transfer difference (STD) NMR methods to map the molecular interactions between the inactivating peptide and its channel target. The results indicate that binding of the ShB peptide to KcsA involves the ortho and meta protons of Tyr[8], which exhibit the strongest STD effects; the C4H in the imidazole ring of His[16]; the methyl protons of Val[4], Leu[7], and Leu[10] and the side chain amine protons of one, if not both, the Lys[18] and Lys[19] residues. When a noninactivating ShB-L7E mutant is used in the studies, binding to KcsA is still observed but involves different amino acids. Thus, the strongest STD effects are now seen on the methyl protons of Val[4] and Leu[10], whereas His[16] seems similarly affected as before. Conversely, STD effects on Tyr[8] are strongly diminished, and those on Lys[18] and/or Lys[19] are abolished. Additionally, Fourier transform infrared spectroscopy of KcsA in presence of ^{13}C-labeled peptide derivatives suggests that the ShB peptide, but not the ShB-L7E mutant, adopts a β-hairpin structure when bound to the KcsA channel. Indeed, docking such a β-hairpin structure into an open pore model for K^+ channels to simulate the inactivating peptide/channel complex predicts interactions well in agreement with the experimental observations.

Inactivation of ion channels limits the duration of channel openings and is essential in shaping and regulating cellular excitability. Early studies on N-type inactivation in voltage-dependent Na^+ or K^+ channels envisioned this process as a consequence of the occlusion of the channel mouth by a flexible cytoplasmic domain, located either at the N-terminal end of the channel protein or at an associated β subunit, which acts as an open channel blocker. This proposal, known as the "ball and chain" hypothesis of channel inactivation (1), received plenty of experimental support, and indeed, several "ball" peptides have been identified in different channels. In the *Shaker* B K^+ channel, the inactivating ball peptide (the ShB peptide) corresponds to the first 20 amino acids of each of the subunits forming the tetrameric channel (MAAVAGLYGLGEDRQHRKKQ) (2, 3). Synthetic peptides derived from the ShB peptide sequence restore inactivation in deletion *Shaker* B channels lacking the inactivation peptide (4) and also inactivate a variety of other K^+ channels (5–10). From such observations it was concluded that channel inactivation has a rather unconstrained basis in terms of primary structure and also that there must be two domains, complementary to those in the ball peptides, configuring the site for the inactivating peptide in the channel protein: (i) a hydrophobic pocket accessible only upon channel opening and separated from the cytoplasm by (ii) a region with a negative surface potential (3, 11). Such conclusions seem supported by the known crystal structures of K^+ channels (12–15) in which the central cavity and inner pore are lined by hydrophobic amino acids, whereas the surrounding cytoplasmic domains contain acidic residues to favor electrostatic interaction with the positively charged C-terminal segment of most ball peptides. Nonetheless, no crystallographic data are yet available on a channel-ball peptide complex, and therefore, issues such as the identity of the peptide-binding site within the channel protein or the conformation adopted by the channel-bound inactivation peptide must await future studies. In the absence of such information, different electrophysiological studies (13, 16) suggest that the inactivating ball peptide snakes into the cytoplasmic channel mouth and stays there during inactivation in an almost linear, extended conformation. On the other hand, the conformational propensity of both the ball peptide of the K_v 3.4 channel (17, 18) and the ShB peptide (19–22) has been studied spectroscopically in solution and in the presence of anionic

* This work was supported by Spanish Ministerio de Educación y Ciencia Grants CTQ2005-00360/BQU (to J. L. N.) and BFU2005-00749 (to J. M. G.-R.); FIPSE Experiment 36557/06 (to J. L. N.) and Grant BANCAJA-UMH IP/UR/01; and Consellería de Empresa, Universidad y Ciencia de la Generalitat Valenciana Grant GV07/017 (to J. A. E.). The costs of publication of this article were defrayed in part by the payment of page charges. This article must therefore be hereby marked "*advertisement*" in accordance with 18 U.S.C. Section 1734 solely to indicate this fact.

[1] These authors contributed equally to this work.
[2] Recipient of a predoctoral fellowship from the Generalitat Valenciana.
[3] Supported in part by predoctoral fellowships from the Ministerio de Educación y Ciencia of Spain.
[4] To whom correspondence should be addressed: Instituto de Biología Molecular y Celular, Edificio Torregaitán, Universidad Miguel Hernández, 03202 Elche (Alicante), Spain. Tel.: 34-966658757; Fax: 34-966658758; E-mail: gonzalez.ros@umh.es.

phospholipid vesicles that, similar to the presumed inactivation site on the channel protein (3, 11), contain a hydrophobic domain (the acyl chains in the lipid bilayer), separated from the aqueous media by the negatively charged vesicle surface. These studies show that ball peptides are poorly structured in solution but adopt a β-structure when challenged by the channel-mimicking model target (19–21). Such β-structure has been identified as a β-hairpin that readily inserts into the hydrophobic domains provided by the lipid bilayer model target (20, 21, 23, 24).

Here we first demonstrate the occurrence of N-type inactivation mediated by the ShB peptide in KcsA, a prokaryotic potassium channel from *Streptomyces lividans* (25). Interestingly, KcsA inactivation is associated to functional uncoupling of channels that exhibited positively coupled gating prior to the addition of the ShB peptide (26). Also, saturation transfer difference (STD)[5] NMR methods (27–29) have been used to identify interactions at atomic resolution in the KcsA-ShB complex. STD spectra are obtained after selective saturation of resonances of the KcsA protein, whereby the magnetization redistributes within the protein via intramolecular spin diffusion. Then, if a bound ligand is present, magnetization transfers from the protein to the ligand via ^{1}H-^{1}H dipolar contacts. An efficient intermolecular magnetization transfer from protons of the protein to the ligand requires very short distances, and therefore, ligand binding is strictly required for the transfer phenomenon. Our results demonstrate that indeed the wild-type ShB peptide binds to KcsA and also distinguish which amino acid residues are involved in binding. Finally, Fourier transform infrared spectroscopy using ^{13}C-labeled ShB peptide supports the notion that the inactivating ShB peptide adopts a β-hairpin structure when channel-bound. Moreover, docking such a β-hairpin into the open channel conformation of KcsA modeled after MthK (14), a prokaryotic channel taken as a model for open K^+ channels, predicts interactions that are well in agreement with those determined in the STD-NMR experiments.

EXPERIMENTAL PROCEDURES

Peptide Synthesis and Characterization—The wild-type ShB and the mutant ShB-L7E peptides were synthesized as C-terminal amidated peptides in an automatic multiple synthesizer (AMS 422, Abimed, Lanfengeld, Germany) by using a solid phase procedure and standard Fmoc chemistry (19). The peptides were also acetylated at their N termini. The peptides were purified by reverse phase HPLC to better than 95% purity, and their composition and molecular mass were confirmed by amino acid analysis and mass spectrometry (19). The residual trifluoroacetic acid used in peptide synthesis and HPLC purification was removed by repeated lyophilization-solubilization in 10 mM HCl. For the synthesis of the ^{13}C-labeled ShB and ShB-L7E peptide analogs, L-alanine-*N*-Fmoc (1-^{13}C, 99%) and L-leucine-*N*-Fmoc (1-^{13}C, 99%) (from Cambridge Isotope Laboratories, Inc.) were used, instead of the regular L-alanine and L-leucine reagents, under otherwise identical experimental procedures.

Protein Expression and Purification—Expression of the wild-type KcsA protein with an added N-terminal hexahistidine tag in *Escherichia coli* M15 (pRep4) cells and its purification by affinity chromatography on a Ni^{2+}-nitrilotriacetic acid-agarose column was carried out as reported (30). The final buffer used with the purified protein was 20 mM Hepes, pH 7.0, containing 100 mM KCl and 1 mM DDM. 1–125 KcsA was prepared by chymotrypsin hydrolysis of wild-type KcsA and characterized by matrix-assisted laser desorption ionization tryptic-peptide mass fingerprinting (30).

Reconstitution of KcsA into Asolectin Lipid Vesicles—Large unilamellar vesicles of asolectin (soybean lipids, type II-S; Sigma) were prepared at 25 mg/ml in 10 mM Hepes, pH 7.5, 100 mM KCl (reconstitution buffer) and stored in liquid N_2 (31). The purified, DDM-solubilized KcsA protein was mixed with the above asolectin vesicles previously resolubilized in 3 mM DDM at a lipid:protein subunit molar ratio of 500:1, for 2 h. Reconstituted liposomes were formed by removing the detergent by gel filtration on Sephadex G-50 (fine, 15–20-ml bed volume) previously swollen overnight in buffer without detergent. The detergent-solubilized lipid/protein mixture (2 ml) was loaded on top of the column, and the reconstituted liposomes were eluted in the void volume. The protein-containing reconstituted fractions were pooled and centrifuged for 30 min at 300,000 $\times$ *g*. The pellet was suspended into reconstitution buffer to a protein concentration of 1 mg/ml, divided into 50-μg aliquots, and stored in liquid N_2 (30).

Electrophysiological Recordings in Reconstituted Giant Liposomes—Multilamellar giant liposomes (up to 50–100 μm in diameter) were prepared by submitting a mixture of the reconstituted vesicles from above (usually containing 50 μg of KcsA protein) and asolectin lipid vesicles (25 mg of total lipids) to a cycle of partial dehydration/rehydration (26, 30, 31). Standard inside-out patch clamp recordings (32) were carried out on excised patches from giant liposomes containing the wild-type KcsA, as reported previously (26). Recordings were obtained using either an Axopatch 200A (Axon Instruments) or an EPC-9 (Heka Electronic, Lambrecht/Pfalzt, Germany) patch clamp amplifier, at a gain of 50 mV/pA. The holding potential was applied to the interior of the patch pipette, and the bath was maintained at virtual ground ($V = V_{bath} - V_{pipette}$). The recordings were filtered at 1 kHz, and the data were analyzed with the Clampfit-9 software (Axon Instruments). An Ag-AgCl wire was used as the reference electrode through an agar bridge. All of the measurements were made at room temperature. The pipette (extracellular) solution contained 10 mM Hepes buffer, pH 7, 100 mM KCl, and the bath (intracellular) solution contained 10 mM MES buffer, pH 4, 100 mM KCl.

Nuclear Magnetic Resonance Spectroscopy—One-dimensional ^{1}H NMR experiments were recorded at 283 K on a Avance Bruker DRX-500 using a *z* axis gradient by using BBO or TXI probeheads. Two-dimensional NMR spectra were recorded in the phase sensitive mode by using the States time proportional phase incrementation method (33). All of the experiments were carried out using the WATERGATE pulse sequence for water suppression

[5] The abbreviations used are: STD, saturation transfer difference; DDM, dodecyl β-D-maltoside; NOE, nuclear Overhauser effect; Fmoc, *N*-(9-fluorenyl)methoxycarbonyl; HPLC, high pressure liquid chromatography; MES, 4-morpholineethanesulfonic acid.

(34). Two-dimensional ^{1}H-^{1}H total correlation spectra were recorded by using a MLEV-17 spin-lock sequence (35) with a mixing time of 80 ms. NOE spectroscopy experiments were recorded with mixing times of 100 and 250 ms. Typically, spectra were acquired with 512 t_1 increments, 2048 data points, and a relaxation delay of 1 s. The spectral width was 6000 Hz in all cases. The spectra were processed using the BRUKER-XWIN-NMR software working on a PC work station. All of the spectra were zero-filled in the F_1 spectral dimension to 1024 data points, and a squared sine bell window function was applied in both dimensions prior to Fourier transformation. Sequential assignments of proton resonances of ShB and ShB-L7E peptides were based on characteristic sequential NOE connectivities between the H_α of a particular residue, and the amide proton of the next residue in the NOE spectra was referred to internal 3-(trimethylsilyl) propionic acid-2,2,3,3-$^2H_4$-sodium salt.

In the STD experiments, 2 mg of freeze-dried peptide were dissolved in 500 μl of buffer (50 mM d_4-acetic acid, 100 mM KCl, 10% D_2O), containing KcsA either reconstituted in asolectin vesicles or solubilized in 5 mM of the detergent DDM. Deuterated acetic acid and its sodium salt were purchased from Sigma. Peptide and KcsA final concentrations were 2 mM and 45 μM, respectively. The one-dimensional ^{1}H STD NMR (27–29) spectra of ShB or ShB-L7E peptides-KcsA complexes were recorded with usually 4000 scans. Selective saturation of protein resonances was set at −3 ppm (on resonance). Control experiments at this frequency showed that the entire protein (either in reconstituted lipid vesicles or solubilized in DDM micelles) can be saturated uniformly and then efficiently used for the STD NMR technique. In this region, the methyl resonances of the protein appear, and irradiation at protein methyl groups has previously been found to yield the most effective saturation (36); furthermore, this frequency is far away from the most up-field shifted methyl protons of the peptides (see Ref. 22 and our own observations), such that no perturbation of this signal can be induced by the selectively shaped pulse. Investigation of the time dependence of the saturation transfer with saturation times ranging from 0.2 to 2.5 s showed that 1.5 s were needed for efficient transfer saturation from the protein to the ligand protons. STD NMR spectra were acquired using a series of equally spaced 50-ms Gaussian-shaped pulses for selective saturation. The radio frequency field strength of the Gaussian-shaped pulses was ~100 Hz, with a 1-ms delay between the pulses. Residual water signal was eliminated by using excitation sculpting procedures (37). A spin-lock sequence was applied before the excitation sculpting sequence to remove the signals of KcsA (27, 38). The reference STD spectra were recorded with the off resonance set at 30 ppm. The saturated spectra were subtracted from the reference spectra via phase cycling. Experiments with ShB-L7E peptide were only carried out with KcsA reconstituted in asolectin vesicles.

To ensure that the observed signals arose from the STD effect, the following controls were carried out. STD-NMR experiments with the on and off resonance frequencies set either at −3 and 30 ppm, respectively, were acquired with samples containing the ShB peptide in the absence of KcsA, either in plain aqueous buffer or in the presence of DDM; the saturation time was 2 s. No signals were present in the difference spectra, indicating that the effects observed in the presence of KcsA were due to true saturation transfer. In addition, we recorded control experiments in a sample of DDM micelles with on and off saturation frequencies set to identical values (either at −3 or 30 ppm). The difference spectra did not contain any signals, proving that good subtraction was achieved.

To allow for comparison among the different signals in the STD experiments, the signal intensities of the different protons were analyzed by the use of the fractional STD amplification factor, which expresses the signal intensity in the STD spectrum, $I_0 - I_{sat}$, as a fraction of an unsaturated reference spectrum, I_0, and the excess of added ligand (28).

$$\text{STD amplification factor} = \frac{(I_0 - I_{sat})}{I_0} \times [\text{ligand excess}] \quad \text{(Eq. 1)}$$

The errors in the STD amplification factor were estimated from the determination of the STD effects measured in two identical samples at 1.5 s and processed simultaneously. The differences obtained were lower than 10% for all the measured resonances.

Fourier Transform Infrared Spectroscopy—Lyophilized aliquots of synthetic peptides, with or without the desired lipid vesicles, were processed in D_2O buffer as reported earlier (20). For the samples containing detergent-solubilized KcsA, both in the presence and in the absence of added ShB or ShB-L7E peptides, aliquots of KcsA in 10 mM Hepes buffer, pH 7.0, 100 mM KCl, and 1 mM DDM were processes as described earlier (39), except that 10 mM acetate buffer, pH 4.0, 100 mM KCl, 1 mM DDM was used for the washings. Routinely, amide I′ bands in these experiments were 0.4 absorbance units or larger.

For spectral acquisition, the aliquots of 20 μl of each sample were placed between a pair of CaF_2 windows separated by a 50-μm-thick mylar spacers and mounted in a Harrick (Ossining, NY) demountable cell. Temperature (~22 °C) was maintained constant with a circulating water bath. The spectra were recorded on a Bruker IF66s instrument equipped with a DTGS detector, and the sample chamber was continuously purged with dry air. A minimum of 600 scans/spectra were taken, averaged, apodized with a Happ-Genzel function, and Fourier-transformed to give a nominal resolution of 2 cm^{-1} (40). Three spectra were recorded for each sample, and the buffer contribution was subtracted. Derivation was performed using a power of 3 and a breakpoint of 0.3. Self-deconvolution was performed using a Lorenztian bandwidth of 18 cm^{-1} and a resolution enhancement factor of 2.0 (39).

Modeling the ShB-KcsA Complex—The modeling of KcsA in the open conformation was done by homology, using the crystal structure at 3.3 Å resolution of the calcium-gated potassium channel MthK as a template (Protein Data Bank code 1LNQ). The multiple sequence alignment was made with CLUSTALW at the European Bioinformatics Institute site and manually supervised (final 24% identity and 40% similarity). The homology modeling was performed in the Swiss-Model Protein Modeling Server at the ExPASy Molecular Biology site. For model refinements, the orientation and optimization of the side chains was carried out in two steps. First, those residues making van

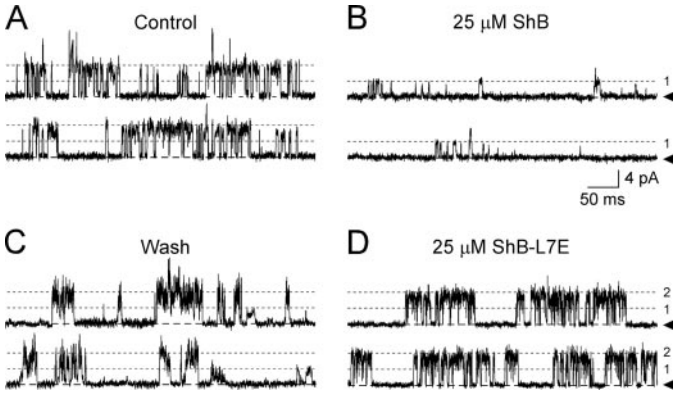

FIGURE 1. **Inactivation of the KcsA channel by the ShB peptide.** The two traces in each panel correspond to different recordings, both taken at +150 mV, for the same experimental condition. *A*, representative control recordings from excised giant liposome patches containing reconstituted KcsA channel displaying the typical activity seen in a low opening probability pattern (26). The channels in such low opening probability patterns of KcsA are closed most of the time and open in bursts of activity, such as shown in the figure. Notice that current levels corresponding mostly to the concerted (coupled) gating of two KcsA channels are observed in these control conditions (26). *B*, addition of the ShB peptide (25 μM) to the solution bathing the patch (cytoplasmic side of the channel) results in the uncoupling of channel gating and in channel inactivation in a peptide concentration-dependent manner. *C*, washing off the added ShB peptide results in the recovery of channel electrical activity and in the reappearance of coupled channel gating. *D*, addition of the noninactivating ShB-L7E peptide (25 μM) to the solution bathing the patch, under otherwise identical conditions to those used in *B*. The *discontinuous line* in all panels and the *arrowheads* indicate the zero current level, whereas the *dotted lines* are indicative of the current levels corresponding to one or two single channel openings.

der Waals' clashes were selected and fitted with "Quick and Dirty" algorithms; second, models were energy minimized (100 steps of steepest descent and 100 conjugate gradient, cut-off of 10 Å for nonbonded interactions) with Insight II (Biosym/MSI, Accelrys Software Inc.). Structure editions were made with Swiss Protein Data Bank viewer v3.7 (41).

The protein-protein docking interaction prediction was accomplished with GRAMM-X v.1.2.0 (42) using default conditions. The protein complex was tested in terms of energy with FoldX (43, 44) at the CRG site and evaluated with PROCHECK (45), showing 81.8% of residues in most favored regions and 17% in additional allowed regions of the Ramachandran plot. The molecular graphic representations were created with PyMOL.

RESULTS AND DISCUSSION

The Inactivating ShB Peptide Uncouples and Inactivates KcsA—The prokaryotic potassium channel KcsA behaves in many respects similarly to its structurally more complex eukaryotic counterparts (46), including the occurrence of slow, C-type inactivation (47). Perhaps for these reasons and also because of the promiscuity of the ShB ball peptide in inducing N-type, rapid inactivation in many different potassium channels (4–10), it has been assumed that the ShB peptide should also induce N-type inactivation in KcsA (13). Nonetheless, no experimental evidence on this matter has been reported to date. Here, we have used patch clamp techniques to study the effects of synthetic ShB peptide on KcsA reconstituted into asolectin giant liposomes. Fig. 1 illustrates the effects of the addition of the ShB peptide to the bath solution (cytoplasmic side of the channel) in an excised, inside-out membrane patch exhibiting a low opening probability pattern, the most frequent functional pattern exhibited by the reconstituted KcsA channel (27). No effects on the ion currents were observed when the ShB peptide was added into the pipette solution (extracellular side of the channel).

Prior to the addition of the peptide (Fig. 1*A*), KcsA exhibits "single channel-like" currents of different sizes (mainly 8 pA, but also a few 12 pA events at +150 mV), which are integer multiples of the smaller, truly KcsA single-channel current of 4 pA, and result from the simultaneous (coupled) gating of two or three KcsA channels (see Ref. 27 for more details on the positive coupling of KcsA). Also, as in the original report on the inactivation of *Shaker* B Δ6–46 channel by the synthetic ShB peptide (4), inactivation of KcsA occurs in a peptide concentration-dependent manner and most noticeably at positive (depolarizing) voltages, where the peptide (Fig. 1*B*) causes only a few, uncoupled 4 pA currents to remain that eventually disappear as the peptide concentration is increased, leaving little or no activity in the recording. An apparently similar uncoupling of channel gating seemed also present in the original report on the effects of the ShB peptide on the *Shaker* B Δ6–46 channel (see Fig. 3 in Ref. 4), although it was not discussed by the authors. On the other hand and also similar to the report on the *Shaker* B channel, only minor effects of the inactivating peptide were observed at negative (up to −200 mV) voltages (not shown). Moreover, Fig. 1*C* shows that washing the ShB peptide off the membrane patch by replacing the bath solution with fresh peptide-free buffer results in the recovery of channel activity and in the reappearance of coupled gating. Finally, no significant effects on the currents are seen at any voltage when, instead of the wild-type ShB peptide, the noninactivating ShB-L7E peptide mutant is used in the experiments (Fig. 1*D*), which is also reminiscent of the original report on the inactivation of the *Shaker* B Δ6–46 channel by ShB peptide derivatives (4).

NMR Assignments and Peptide Structure—The above demonstration that the ShB peptide induces N-type inactivation of the KcsA channel, along with the fact that both the channel and the synthetic peptide can be prepared easily and in sufficiently large amounts, makes this an unique experimental system to learn on the molecular interactions behind the rapid inactivation phenomena through the application of spectroscopic techniques. Here, we have used STD-NMR methods in an attempt to explore such interactions between the inactivating peptide and KcsA as the ion channel target. To this end, we first assigned the resonances seen in the proton NMR spectra of the wild-type ShB peptide in aqueous solution at pH 5.0. Such acidic conditions (pH 4–5.5) have been reported as optimal for opening the KcsA channel (27, 46, 48–51), and indeed, the inactivation patch clamp experiments from above were conducted at pH 4 in the solution bathing the membrane patches. Proton assignment was carried out by using homonuclear standard two-dimensional total correlation spectroscopy and NOE spectroscopy experiments (52). Chemical shifts essentially agreed with those reported previously by Kalbitzer and co-workers at pH 7.2 (see Table 1 in Ref. 22), except for small changes in the side chains of the amino acid His^{16} and its neighboring residues, probably because of protonation of the imid-

azole ring at the acidic pH used here. Under our experimental conditions and in apparent agreement with previous reports (22), the ShB peptide in aqueous solution adopts a mainly disordered conformation, as concluded from: (i) the absence of medium or long range NOEs (Fig. 2*A*); (ii) the small H_α conformational shifts that, with the exception of residues D13 to Gln^{15}, are within the usually accepted limits for random coil conformations (Fig. 2*B*) (53, 54); and (iii) the absence of chemical shift dispersion in both the amide and the methyl group regions of the spectra (data not shown).

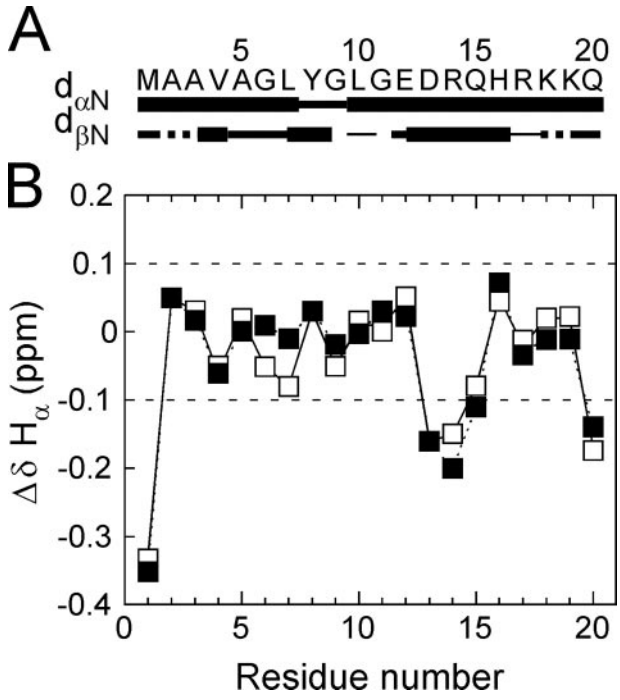

FIGURE 2. **Summary of NMR data and conformational shifts for the ShB peptides.** *A*, sequential NOEs between different atoms of successive residues ($d_{\alpha N}$, $H_\alpha(i)$ − HN(i + 1), and $d_{\beta N}$, $H_\beta(i)$ − HN(i + 1)) for the wild-type ShB peptide. NOEs are classified into strong, medium, or weak, according to the thickness of the *bar* underneath the sequence, and their intensity was judged by visual inspection in the spectra. The *dotted lines* indicate ambiguous observed NOEs caused by spectral overlapping. *B*, conformational shifts of the H_α protons for the wild-type ShB (*blank squares*) and ShB-L7E (*filled squares*) peptides. The resonances of Lys^{18} and Lys^{19} could not be unambiguously assigned. The *dashed lines* indicate the usually accepted range of deviations from random coil conformational shifts.

In the presence of KcsA reconstituted into asolectin vesicles, the spectrum of the ShB peptide experienced a significant line broadening with compared with that in solution, although the chemical shifts of the different protons were not modified (data not shown). We interpret such broadening as a clear indication of an interaction between ShB and KcsA, particularly because it occurs at a high ShB peptide to KcsA molar ratio (2 mM of peptide *versus* 45 μM of KcsA), where the spectral features are dominated by signals arising mostly from the free form of the peptide. Interestingly, either in aqueous solution or in the presence of KcsA reconstituted into asolectin vesicles, the methyl protons of Val^4 appeared at the same chemical shift (0.98 ppm), but those of Leu^7 (0.85 and 0.91 ppm) and Leu^{10} (0.93 and 1.00 ppm) appeared at different chemical shifts, suggesting some preferred local orientations, as reported in other random coil ensembles (53, 54).

Proton assignments were also obtained for the noninactivating ShB-L7E mutant peptide both in aqueous solution and in the presence of KcsA reconstituted into lipid vesicles. In either condition, the ShB-L7E peptide showed similar chemical shifts to those exhibited by the wild-type ShB peptide, except for amino acids Gly^6 and Tyr^8, which are adjacent to the mutation site. Despite the similarities, two observations were made in the ShB-L7E peptide that differed from those made in the wild-type ShB. First, the line broadening of peptide signals observed in the presence of KcsA was not as large as that observed for the wild-type ShB (Fig. 3, *A* and *B*), suggesting a weaker binding of the ShB-L7E peptide to the KcsA channel. Second, the resonances of the methyl groups of Leu^{10} were degenerated in the ShB-L7E, suggesting that the preferred local conformation observed in the wild-type ShB peptide around these methyl groups is disrupted in the noninactivating mutant.

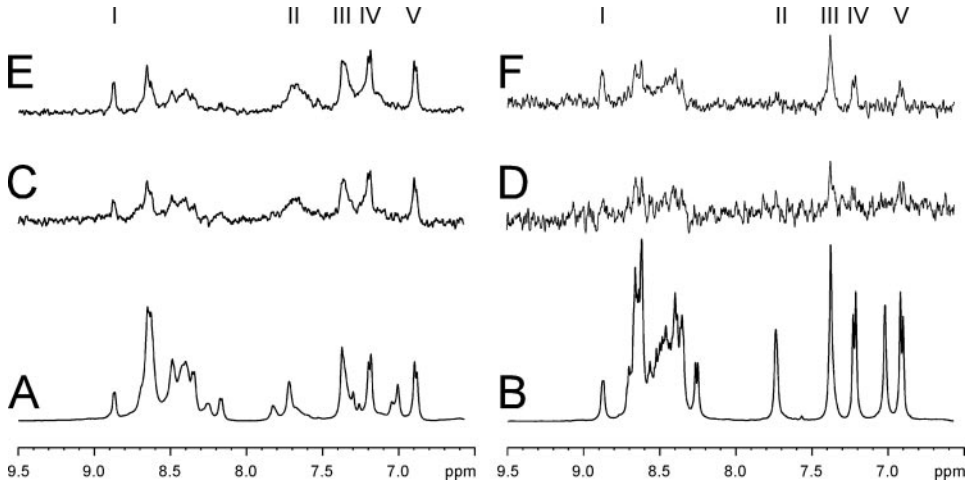

FIGURE 3. **STD in the interaction of KcsA and the peptides ShB (*left side*) and ShB-L7E (*right side*).** *A* and *B* show the reference spectra of ShB and ShB-L7E, respectively, in the presence of KcsA reconstituted into asolectin vesicles. *C* and *D* show the STD-NMR spectrum after a saturation of 1 s, whereas *E* and *F* show the STD-NMR spectrum at a saturation time of 2.5 s. In *C–F*, KcsA resonances were selectively saturated by irradiation at −3 ppm. The *roman numerals* indicate the proton resonances from the different amino acids showing strong STD effects: *I*, amide proton of Ala^2; *II*, the side chain NH protons of Lys^{18} and/or Lys^{19} (7.70 ppm); *III*, the C4H of His^{16} (7.36 ppm); *IV*, the ortho protons of Tyr^8 (7.20 ppm); *V*, meta proton of Tyr^8 (6.88 ppm). The peptide concentration was 2 mM, whereas the concentration of KcsA reconstituted in asolectin vesicles was 45 μM in 50 mM acetic/acetate, 100 mM KCl, pH 5.5.

Probing Wild-type ShB Peptide-KcsA Channel Interactions in STD-NMR Experiments—Fig. 3 shows the amide region of a reference, nonsaturated ^{1}H NMR spectrum of a sample containing the wild-type ShB peptide and KcsA reconstituted into asolectin vesicles (Fig. 3*A*), along with STD-NMR spectra from the same sample, taken at different times of saturation (1 s, *panel C* and 2.5 s, *panel E*). Several resonances can be observed within the one-dimensional ^{1}H-STD NMR spectra, which (i) are sufficiently resolved from the rest of the peptide reso-

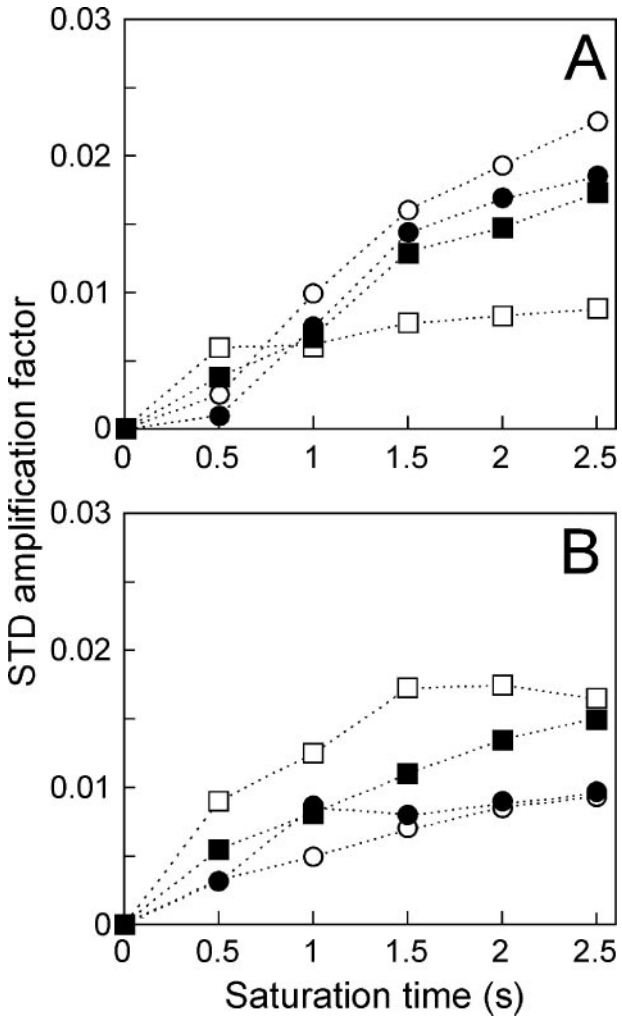

FIGURE 4. **STD amplification factors for ShB and ShB-L7E.** The STD amplification factors at different saturation times were calculated for the interaction of wild-type ShB (*A*) and ShB-L7E (*B*) to KcsA reconstituted into asolectin lipid vesicles. The different symbols correspond to the ortho (*blank circles*) and meta (*filled circles*) protons of Tyr^{8}; the methyl protons of Val^{4}, Leu^{7} (not present in ShB-L7E), and Leu^{10} (*blank squares*); and the C4H proton of the imidazole ring of His^{16} (*filled squares*). The errors at each experimental point were lower than 10%, as concluded from two different experimental series of STD measurements.

nances as to be accurately monitored and (ii) show changes in the intensity of the STD signals with the different times of saturation used in the experiments (Fig. 4*A*). In particular, the ortho (at 7.20 ppm) and meta (at 6.88 ppm) protons of Tyr^{8} are among the ShB peptide resonances showing the largest STD effects. This seems consistent with previous findings indicating that Tyr^{8} is a critical residue for the ShB peptide to retain its ability to inactivate channels, as well as to adopt a defined, β-hairpin conformation upon binding to anionic phospholipid vesicles, a model target mimicking some of the presumed features of the inactivating peptide-binding site on the channel protein (23, 55). Interestingly, a conservative Y8F mutation was shown to retain the ability of the wild-type peptide to inactivate potassium channels (16), thus lending support to our findings that the protons at the bulky aromatic ring of Tyr^{8} are important in the interaction of the peptide with the target channel during inactivation.

We also observed a strong STD effect on the C4H of the imidazole ring of His^{16} (at 7.36 ppm), as well as a much weaker STD effect on the amine protons of the side chains of Lys^{18} and/or Lys^{19} (at ~7.70 ppm and close to one of the protons of the side chains of Gln^{15} and Gln^{20}). Finally, the amide proton of Ala^{2} (at 8.85 ppm) also shows STD effects, but they were smaller than any other described here and will no be further discussed. Moreover, the methyl protons of Val^{4}, Leu^{7}, and Leu^{10} also experienced significant STD effects (Fig. 4), although their magnitude was not as large as those observed for the aromatic protons of Tyr^{8}. Taken together, the above results indicated that binding of the ShB peptide to KcsA reconstituted into lipid vesicles involved mainly the aromatic rings of both Tyr^{8} and His^{16} in the inactivating peptide.

When the experiments were performed using DDM-solubilized KcsA as the target for the ShB peptide, instead of the reconstituted KcsA vesicles, a similar line broadening of the ShB peptide signals was observed. Moreover, practically identical STD effects were seen in such samples, suggesting that KcsA in the detergent-solubilized form is as capable as the reconstituted KcsA in allowing binding of the ShB peptide. Unfortunately, however, the presence of signals in the aliphatic region arising from the detergent overlapped with some of the peptide signals, thus preventing an adequate integration. Therefore, we decided not to study any further the detergent-solubilized system.

STD-NMR Monitoring of the Interaction of the Noninactivating ShB-L7E Peptide with KcsA Reconstituted into Lipid Vesicles—As concluded from the above patch clamp experiments, the ShB-L7E peptide does not inactivate the KcsA channel, which also resembles the original observation by Aldrich and co-workers (4) on the *Shaker* B Δ6–46 channel. Interestingly, despite such dramatic functional differences between the noninactivating ShB-L7E peptide and the wild-type ShB, both peptides are able to bind to the KcsA channel, as suggested by the line broadening observed in the NMR spectral bands (see above). However, the STD effects are quite different from those observed in the ShB peptide (Figs. 3 and 4). For instance, the STD effects on the aromatic protons of Tyr^{8} are clearly smaller in the mutant ShB-L7E peptide than in the wild-type ShB peptide. Conversely, STD effects on the methyl groups of Val^{4} and Leu^{10} are clearly more important in the mutant peptide than in its wild-type counterpart, despite the fact that in the latter, this contribution includes also that of Leu^{7}, which is obviously lacking in the mutant L7E peptide (Fig. 4). Furthermore, the side chains of Lys^{18} and/or Lys^{19} displayed STD effects in the wild-type ShB peptide but do not give rise to any STDs in the ShB-L7E peptide, indicating that the side chains of these residues do not participate in the binding of the mutant peptide to KcsA. Therefore, the main conclusion from these experiments is that binding of the noninactivating ShB-L7E peptide to KcsA results in less important STD effects on the key residue Tyr^{8}, as well as none at all on Lys^{18} and/or Lys^{19}, being the interaction between the KcsA protein with the aliphatic Val^{4} and Leu^{10} methyl groups clearly more intense. Finally, the involvement of the aromatic moiety of His^{16} in the binding to the channel protein remains similar, within experimental error, for both peptides.

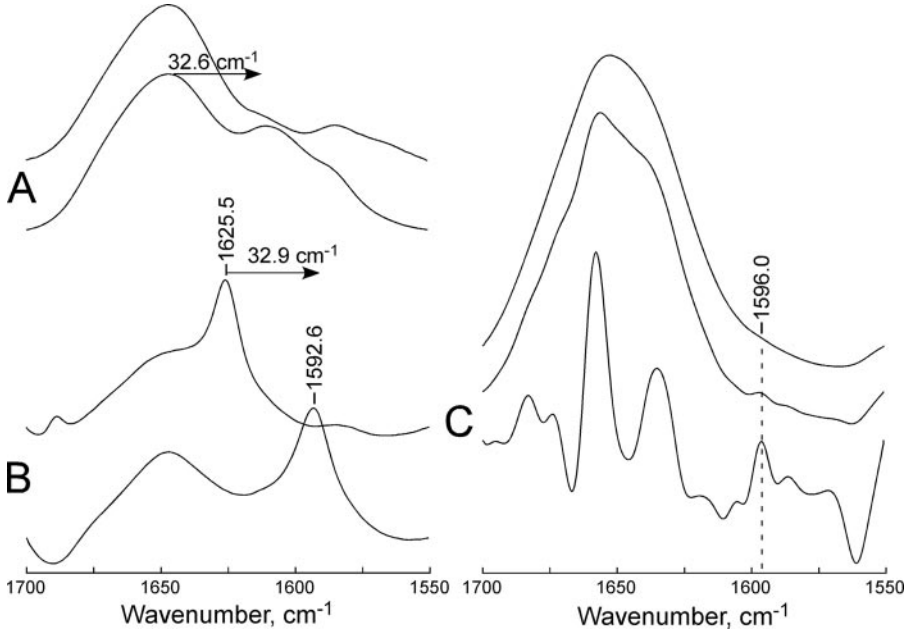

FIGURE 5. **Infrared studies on the conformation of ShB bound to KcsA.** *A* and *B* show the amide I′ infrared spectral region of the ShB peptide in plain buffer (10 mM Hepes, pH 7, 100 mM NaCl) (*A*) as well as in the presence of dimyristoyl phosphatidic acid vesicles (*B*), under otherwise identical conditions. The *lower traces* in both panels correspond to the ^{13}C-labeled ShB peptide derivative, while the *upper traces* correspond to the nonlabeled, wild-type ShB. *C* shows the infrared spectrum of a sample containing a mixture of ^{13}C-labeled ShB peptide and DDM-solubilized KcsA at a 1:1 molar ratio of peptide per KcsA subunit in acetate buffer, pH 4, 100 mM KCl, 5 mM DDM. The *upper trace* is the original spectrum, whereas the *middle* and *lower traces* represent the Fourier self-deconvolution and derivative of the spectrum, respectively.

Does the ShB Peptide Adopt a Defined Conformation when Bound to the KcsA Channel?—The above NMR measurements suggested that the inactivating ShB peptide and the noninactivating ShB-L7E peptide mutant associate in different manners to the KcsA channel protein. Hypothetically, such a different association could be due to the adoption of different conformations by the peptides once they become channel-bound. Thus, we thought of characterizing such putative peptide structures by means of NOE transfer measurements (56). Unfortunately, however, no such transfer NOEs could be obtained, even when employing different channel to peptide ratios (ranging from 45:1 to 15:1, in molar terms) and mixing times (ranging from 100 to 400 ms). Detection of transfer NOEs requires a fast exchange between free and bound forms of the peptide ligand (57), and therefore, it is conceivable that they could not be detected here, because of an unfavorable slow exchange of the ligand from the ShB-KcsA complex. This could perhaps be the case, because the dissociation constant estimated from fluorescence titrations of the binding of ShB peptide to the KcsA channel is of $\sim 4 \times 10^{-7}$ M.[6] Whatever the reason might be, we turned out to conformation-sensitive Fourier transform infrared spectroscopy measurements as an alternative means to detect the possible adoption of a defined structure by the ShB peptide upon interaction with the KcsA channel. For technical simplicity, because the interaction of ShB with KcsA reconstituted into asolectin vesicles is similar to that seen in detergent solution (see above), the Fourier transform infrared spectroscopy measurements were carried out on detergent-solubilized channel/peptide mixtures. Also, the chymotryptic derivative 1–125 KcsA was used in these experiments instead of the wild-type channel, because it was found that cleavage of the cytoplasmic C terminus facilitated channel inactivation by the ShB peptide and allows the use of lower peptide concentrations.[7] Finally, because the relevant infrared bands in both the peptide and the channel protein are fully overlapped, we performed these experiments using a heavy isotope-labeled ShB peptide, in which all the alanine (Ala^2, Ala^3, and Ala^5) and leucine (Leu^7 and Leu^{10}) residues were substituted by their 1-^{13}C analogs. Under such conditions, an isotopic shift to lower vibrational frequencies in the infrared bands of the heavy isotope-labeled peptide is expected, which should permit its monitoring separately from the spectral bands arising from the nonlabeled channel protein or other sample components.

Fig. 5*A* shows that the amide I′ band of the nonlabeled ShB peptide in aqueous solution, where the peptide is known to adopt a random conformation (see above) (20), is indeed dominated by a 1644 cm^{-1} spectral component, assigned to nonordered secondary structure. In the ^{13}C-labeled peptide, an additional shoulder at 1610 cm^{-1} was observed, thus allowing for the separate detection of $^{12}C{=}O$ and $^{13}C{=}O$ vibrations, which differed in $\sim$33 cm^{-1}. Such extent in the isotopic shift was further confirmed by spectra of the ShB peptide taken in the presence of anionic lipid (dimyristoyl phosphatidic acid) vesicles (Fig. 5*B*), which is known to induce the adoption of a β-hairpin structure in the ShB peptide with a characteristic band at 1624 cm^{-1} (20). In the ^{13}C-labeled peptide, this spectral component was shifted to $\sim$1593 cm^{-1} (Fig. 5*B*). Similar results were obtained with DMPG vesicles (data not shown). Interestingly, the spectra of the labeled ShB peptide in the presence of anionic lipid vesicles showed little or none of the nonlabeled β-hairpin band at 1624 cm^{-1}, suggesting that the amino acid residues substituted by their ^{13}C-labeled counterparts are precisely those contributing the most to the observed β-hairpin peptide structure.

Fig. 5*C* shows the results obtained when using the ^{13}C-labeled ShB peptide in presence of the KcsA channel. Despite the extent of the isotopic shift from above, the amide I′ band arising from the detergent-solubilized KcsA is too large and still overlaps considerably with the spectral region where the amide I′ band from the ^{13}C-labeled ShB peptide is expected to appear (Fig. 5, *A* and *B*). Nevertheless, despite overlapping, use of res-

[6] F. N. Barrera, unpublished observation.

[7] M. L. Molina, unpublished observation.

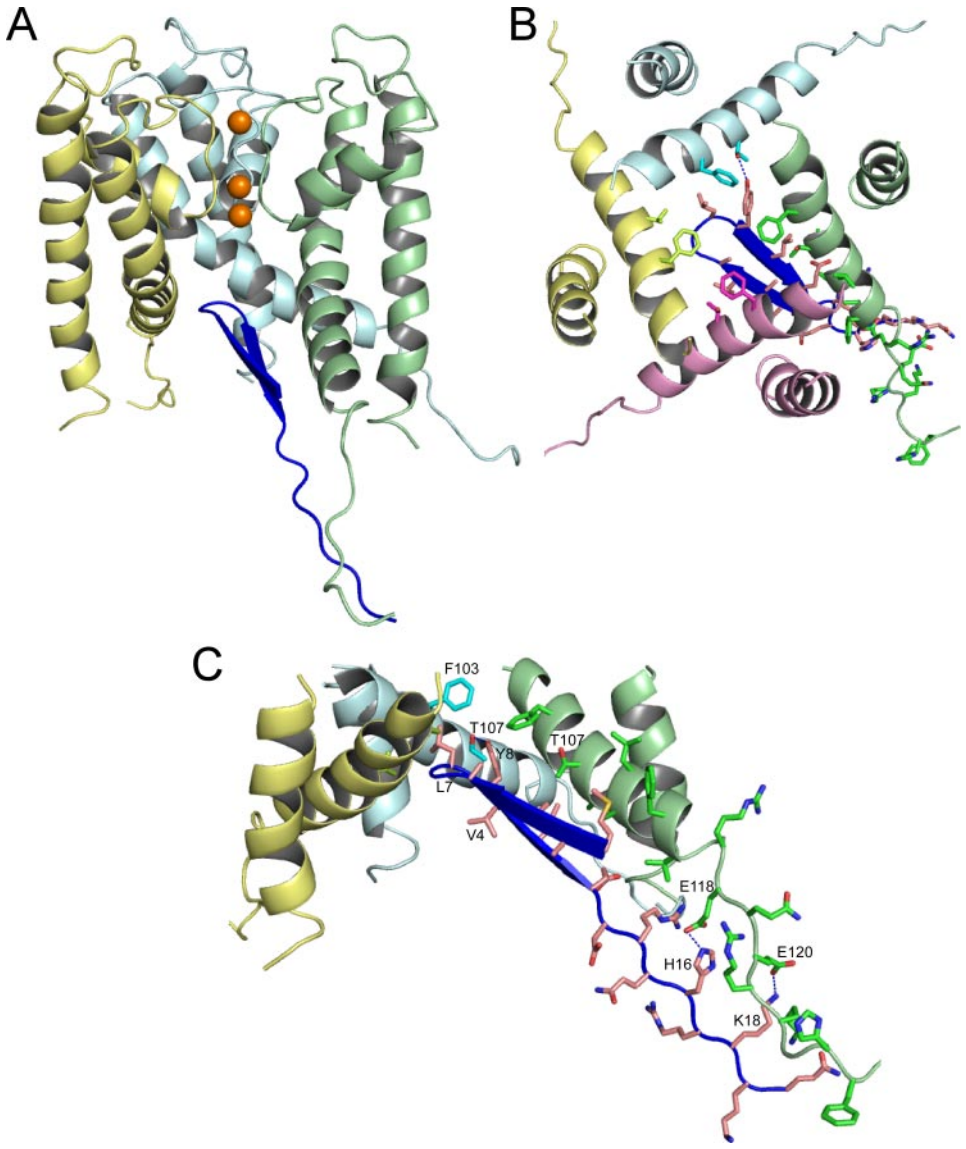

FIGURE 6. **Structural model of the ShB peptide/KcsA channel complex as obtained by GRAMM (see "Experimental Procedures" for details).** The ShB peptide has been modeled as a β-hairpin, as reported previously (21), whereas modeling of KcsA in the open conformation has been done by homology, using the crystal structure at 3.3 Å resolution of the calcium-gated potassium channel MthK as the template (14) (Protein Data Bank code 1LNQ). *A* shows a side view of the complex in which one of the KcsA subunits has been removed to facilitate the observation. The ShB peptide is drawn in *dark blue*, whereas three potassium ions inside the selectivity filter appear in *brown*. *B* is a top view zooming of part of the internal vestibule of the peptide/channel complex, as viewed down from the N-terminal end of the selectivity filter. The side chains of Phe103 and Thr^{107} have been drawn to indicate that those two residues from the four KcsA subunits make up the site of interaction for most of the hairpin moiety of the ShB peptide. *C* is a side view zooming on the putative interactions between the C-terminal moiety of the ShB peptide and the initial part of the cytoplasmic, C-terminal domain of KcsA that follows the TM2 transmembrane fragment. Again, in this panel we have removed one of the KcsA subunits for clarity. Binding energy calculation on the model structure shown in the figure yields values of 7.75 Kcal/mol, corresponding to a dissociation constant of ~2 μM.

olution enhancement techniques, such as Fourier self-deconvolution or derivation, allowed the detection of a spectral component at ~1596 cm^{-1}, *i.e.* at approximately the same wave number corresponding to the β-hairpin structure detected in the ^{13}C-labeled ShB peptide (Fig. 5*B*). The 1596 cm^{-1} component was not found in control experiments (i) where the ^{13}C-labeled peptide was dissolved either in detergent micelles or in the presence of asolectin vesicles without KcsA or (ii) when a ^{13}C-labeled ShB-L7E peptide was used in the experiments instead of the wild-type derivative (data not shown). Therefore, despite the difficulties arising from spectral overlap, we interpret such spectral component as truly derived from the acquisition of a β-hairpin or similar structure by a presumably small population of ^{13}C-labeled-ShB peptide bound to the KcsA channel during the course of the experiment. A potential candidate for such a structure could be the β-turn resulting from Asp^{13}, Arg^{14}, and Gln^{15}, as suggested by the slight deviation from the accepted random coil conformational shifts. This, however, seems unlikely because the only ^{13}C-labeled residue near such putative turn is Leu^{10}, which should not be able to produce the infrared component seen at 1596 cm^{-1}. A more likely possibility is that such structure corresponds to a β-turn similar to that causing the β-hairpin seen when the ShB peptide is confronted to anionic lipid vesicles, a much simpler experimental model system mimicking certain physicochemical features of the cytoplasmic channel mouth (21). This seems supported by the similarity observed in the wave number of the spectral components seen in the ^{13}C-ShB when bound to the KcsA channel (1596 cm^{-1}) and in the ^{13}C-ShB peptide in presence of anionic lipid vesicles (1593 cm^{-1}). Furthermore, the β-hairpin structures resulting from a β-turn either at VAGL (residues 4–7) or at AGLY (residues 5–8) (21) include hydrogen bonding of all the ^{13}C-labeled amino acid residues in ShB, namely, Ala^2, Ala^3, Ala^5, Leu^7, and Leu^{10}, thus making it possible to produce the observed 1596 cm^{-1} component in the infrared spectrum. In either case, the putative β-hairpins would define a mostly hydrophobic domain comprising the N-terminal half of the ShB peptide that, as indicated in the Introduction section, should have a complementary domain into the cytoplasmic channel mouth, into which it should be able to enter and bind when the channel is in the open state. Size seems not to be a problem, because the width of a β-hairpin would not exceed that of the cytoplasmic mouth of KcsA (14).

In an attempt to integrate the above experimental information, we carried out docking of the ShB peptide modeled as a β-hairpin, into an open channel conformation of KcsA modeled after the x-ray structure of MthK, the open K^+ channel

model (Fig. 6). The amino acid residues indicated in the figure and their numbering correspond to the KcsA sequence after the homology alignment on the MthK sequence. Fig. 6*A* shows that the ShB hairpin predictably enters into the pore up to the hydrophobic pocket provided mainly by the Phe^{103} and Thr^{107} residues from all four KcsA subunits, ~8–9 Å below the N-terminal end of the selectivity filter. The docking model foresees interactions involving Val^4, Leu^7, Tyr^8, and Leu^{10} in the ShB peptide and Phe^{103} and Thr^{107} in KcsA (Fig. 6*B*). Likewise, the model predicts that His^{16} and possibly Lys^{18} in the ShB peptide may be hydrogen-bonded to Glu^{118} and Glu^{120}, respectively, in the KcsA channel (Fig. 6*C*). Interestingly, the energy estimates for the modeled ShB peptide/KcsA channel complex yield binding affinities in the micromolar range, similar to that determined experimentally by patch clamp measurements. Moreover, a previous report based on a double mutant cycle analysis (13) using the α subunit of rat K_v 1.4 channel, a mammalian homolog of *Shaker*, and the construct β 12 subunit as the inactivation gate, predicted that peptide binding to the channel should involve the residues equivalent to Ala^3, Gly^6, or Leu^7 in the ShB peptide and Thr^{107} or Ala^{111} in the KcsA channel, which is in apparent agreement with our expectations from the docking model. Thus, the predictions from the docking model seem consistent with the experimental data and lend further support to both the identity of the amino acid residues conforming the ShB peptide-binding epitope and the adoption of the β-hairpin conformation when the inactivating peptide is channel-bound.

Conclusions and Final Remarks—Rapid inactivation of KcsA, a prokaryotic potassium channel, by a synthetic peptide (the ShB peptide) having the sequence of the inactivating ball peptide of the eukaryotic *Shaker* B K^+ channel is reported. We found that channel inactivation is associated to functional uncoupling of positively coupled KcsA channels and exhibits similar features to those reported originally for the inactivation by the ShB peptide of *Shaker* and other K^+ channels of eukaryotic origin. Such similarity emphasizes the conservation through evolution of important functional domains in these channels and further confirms KcsA as a *bona fide* model for studying potassium channels.

This report also introduces STD-NMR methods to study ion channel inactivation, drawing important information on molecular events that were largely unknown up to now. Thus, it is observed that regardless of whether the wild-type ShB peptide or the noninactivating ShB-L7E mutant peptide is used in the experiments, there is always peptide binding to the KcsA channel. However, clear differences in the binding of both peptides to KcsA were detected. For instance, Tyr^8 in the ShB peptide displays a stronger interaction with KcsA than its homolog Tyr^8 in the noninactivating ShB-L7E peptide. Furthermore, qualitative differences were observed for the side chains of Lys^{18} and/or Lys^{19}, because the STDs observed for these residues in the ShB peptide were not observed in the ShB-L7E peptide. Finally, the STD effects obtained for the methyl groups of Val^4 and Leu^{10} were clearly more intense in the mutant than in the wild-type peptide. These results indicate that the mutation at position 7 alters not only the binding of the peptide to the KcsA channel, but also the topology of the peptide atoms within the KcsA binding site. Unfortunately, transfer NOEs could not be obtained, and therefore, the adoption of preferred conformations by either peptide when bound to the KcsA channel could not be assessed by means of NMR. On the contrary, Fourier transform infrared spectroscopy measurements using ^{13}C-labeled peptides could be applied successively, and although not fully conclusive because of spectral overlap, they suggest that the ShB peptide, but not the noninactivating ShB-L7E mutant, adopts a β-hairpin structure when bound to the KcsA channel. Indeed, such conclusions seem supported by the observations derived from docking the ShB peptide as a β-hairpin into a KcsA open channel model, which predicts the occurrence or interactions very similar to those observed experimentally.

Acknowledgments—We thank Prof. Alain Milon (Institut de Pharmacologie et de Biologie Structurale, CNRS, Toulouse, France) for helpful comments on the possible uses of STD-NMR prior to the initiation of this work; Prof. Gloria Riquelme (Instituto de Ciencias Biomédicas, Facultad de Medicina, Universidad de Chile) for continuous support and advice on the patch clamp studies; and Alicia Hurtado for involvement in spectral assignment. May García, María del Carmen Fuster, Javier Casanova, María T. Garzón, Helena López, and Eva Martínez provided excellent technical assistance throughout.

REFERENCES

1. Armstrong, C. M., and Bezanilla, F. (1977) *J. Gen. Physiol.* **70,** 567–590
2. Hoshi, T., Zagotta, W. N., and Aldrich, R. W. (1990) *Science* **250,** 533–538
3. Catterall, W. A. (1995) *Annu. Rev. Biochem.* **64,** 493–531
4. Zagotta, W. N., Hoshi, T., and Aldrich, R. W. (1990) *Science* **250,** 568–571
5. Isacoff, E. Y., Jan, Y. N., and Jan, L. Y. (1991) *Nature* **353,** 86–90
6. Dubinsky, W. P., Mayorga-Wark, O., and Schultz, S. G. (1992) *Proc. Natl. Acad. Sci. U. S. A.* **89,** 1770–1774
7. Riquelme, G., Fernandez, A. M., Encinar, J. A., Gonzalez-Ros, J. M., and Sepulveda, F. V. (1999) *Pfluegers Arch. Eur. J. Physiol.* **438,** 879–882
8. Toro, L., Stefani, E., and Latorre, R. (1992) *Neuron* **9,** 237–245
9. Foster, C. D., Chung, S., Zagotta, W. N., Aldrich, R. W., and Levitan, I. B. (1992) *Neuron* **9,** 229–236
10. Kramer, R. H., Goulding, E., and Siegelbaum, S. A. (1994) *Neuron* **12,** 655–662
11. Kukuljan, M., Labarca, P., and Latorre, R. (1995) *Am. J. Physiol.* **268,** C535–C556
12. Doyle, D. A., Morais, C. J., Pfuetzner, R. A., Kuo, A., Gulbis, J. M., Cohen, S. L., Chait, B. T., and MacKinnon, R. (1998) *Science* **280,** 69–77
13. Zhou, M., Morais-Cabral, J. H., Mann, S., and MacKinnon, R. (2001) *Nature* **411,** 657–661
14. Jiang, Y., Lee, A., Chen, J., Cadene, M., Chait, B. T., and MacKinnon, R. (2002) *Nature* **417,** 523–526
15. Long, S. B., Tao, X., Campbell, E. B., and MacKinnon, R. (2007) *Nature* **450,** 376–382
16. Murrell-Lagnado, R. D., and Aldrich, R. W. (1993) *J. Gen. Physiol.* **102,** 949–975
17. Antz, C., Geyer, M., Fakler, B., Schott, M. K., Guy, H. R., Frank, R., Ruppersberg, J. P., and Kalbitzer, H. R. (1997) *Nature* **385,** 272–275
18. Abbott, G. W., Mercer, E. A., Miller, R. T., Ramesh, B., and Srai, S. K. (1998) *Biochemistry* **37,** 1640–1645
19. Fernandez-Ballester, G., Gavilanes, F., Albar, J. P., Criado, M., Ferragut, J. A., and Gonzalez-Ros, J. M. (1995) *Biophys. J.* **68,** 858–865
20. Encinar, J. A., Fernandez, A. M., Gavilanes, F., Albar, J. P., Ferragut, J. A., and Gonzalez-Ros, J. M. (1996) *Biophys. J.* **71,** 1313–1323
21. Encinar, J. A., Fernandez, A. M., Gil-Martin, E., Gavilanes, F., Albar, J. P., Ferragut, J. A., and Gonzalez-Ros, J. M. (1998) *Biochem. J.* **331,** 497–504
22. Schott, M. K., Antz, C., Frank, R., Ruppersberg, J. P., and Kalbitzer, H. R.

(1998) *Eur. Biophys. J.* **27,** 99–104
23. Encinar, J. A., Fernandez, A. M., Poveda, J. A., Molina, M. L., Albar, J. P., Gavilanes, F., and Gonzalez-Ros, J. M. (2003) *Biochemistry* **42,** 8879–8884
24. Hong, S. Y., Oh, J. E., and Lee, K. H. (1999) *Biochem. Pharmacol.* **58,** 1775–1780
25. Schrempf, H., Schmidt, O., Kummerlen, R., Hinnah, S., Muller, D., Betzler, M., Steinkamp, T., and Wagner, R. (1995) *EMBO J.* **14,** 5170–5178
26. Molina, M. L., Barrera, F. N., Fernandez, A. M., Poveda, J. A., Renart, M. L., Encinar, J. A., Riquelme, G., and Gonzalez-Ros, J. M. (2006) *J. Biol. Chem.* **281,** 18837–18848
27. Mayer, M., and Meyer, B. (1999) *Angew. Int. Chem. Int. Ed.* **38,** 1784–1788
28. Mayer, M., and Meyer, B. (2001) *J. Am. Chem. Soc.* **123,** 6108–6117
29. Klein, J., Meinekee, R., Mayer, M., and Meyer, B. (1999) *J. Am. Chem. Soc.* **121,** 5336–5337
30. Molina, M. L., Encinar, J. A., Barrera, F. N., Fernandez-Ballester, G., Riquelme, G., and Gonzalez-Ros, J. M. (2004) *Biochemistry* **43,** 14924–14931
31. Riquelme, G., Lopez, E., Garcia-Segura, L. M., Ferragut, J. A., and Gonzalez-Ros, J. M. (1990) *Biochemistry* **29,** 11215–11222
32. Hamill, O. P., Marty, A., Neher, E., Sakmann, B., and Sigworth, F. J. (1981) *Pfluegers Arch. Eur. J. Physiol.* **391,** 85–100
33. States, D. J., Haberkorn, R. A., and Ruben, D. J. (1982) *J. Magn. Reson.* **48,** 286–292
34. Piotto, M., Saudek, V., and Sklenar, V. (1992) *J. Biomol. NMR* **2,** 661–665
35. Bax, A., and Davis, D. G. (1985) *J. Magn. Reson.* **65,** 355–360
36. Yan, J., Kline, A. D., Mo, H., Shapiro, M. J., and Zartler, E. R. (2003) *J. Magn Reson.* **163,** 270–276
37. Prost, E., Sizun, P., Piotto, M., and Nuzillard, J. M. (2002) *J. Magn Reson.* **159,** 76–81
38. Meyer, B., and Peters, T. (2003) *Angew. Chem. Int. Ed. Engl.* **42,** 864–890
39. Encinar, J. A., Molina, M. L., Poveda, J. A., Barrera, F. N., Renart, M. L., Fernandez, A. M., and Gonzalez-Ros, J. M. (2005) *FEBS Lett.* **579,** 5199–5204
40. Fernandez-Ballester, G., Castresana, J., Arrondo, J. L., Ferragut, J. A., and Gonzalez-Ros, J. M. (1992) *Biochem. J.* **288,** 421–426
41. Guex, N., and Peitsch, M. C. (1997) *Electrophoresis* **18,** 2714–2723
42. Tovchigrechko, A., and Vakser, I. A. (2006) *Nucleic Acids Res.* **34,** 310–314
43. Guerois, R., Nielsen, J. E., and Serrano, L. (2002) *J. Mol. Biol.* **320,** 369–387
44. Schymkowitz, J., Borg, J., Stricher, F., Nys, R., Rousseau, F., and Serrano, L. (2005) *Nucleic Acids Res.* **33,** 382–388
45. Laskowski, R. A., Rullmannn, J. A., MacArthur, M. W., Kaptein, R., and Thornton, J. M. (1996) *J. Biomol. NMR* **8,** 477–486
46. LeMasurier, M., Heginbotham, L., and Miller, C. (2001) *J. Gen. Physiol.* **118,** 303–314
47. Cordero-Morales, J. F., Jogini, V., Lewis, A., Vasquez, V., Cortes, D. M., Roux, B., and Perozo, E. (2007) *Nat. Struct. Mol. Biol.* **14,** 1062–1069
48. Meuser, D., Splitt, H., Wagner, R., and Schrempf, H. (1999) *FEBS Lett.* **462,** 447–452
49. Splitt, H., Meuser, D., Borovok, I., Betzler, M., and Schrempf, H. (2000) *FEBS Lett.* **472,** 83–87
50. Heginbotham, L., LeMasurier, M., Kolmakova-Partensky, L., and Miller, C. (1999) *J. Gen. Physiol.* **114,** 551–560
51. Cuello, L. G., Romero, J. G., Cortes, D. M., and Perozo, E. (1998) *Biochemistry* **37,** 3229–3236
52. Wüthrich, K. (1986) *NMR of Proteins and Nucleic Acids*, Wiley-Interscience, New York
53. Neri, D., Billeter, M., Wider, G., and Wuthrich, K. (1992) *Science* **257,** 1559–1563
54. Evans, P. A., Topping, K. D., Woolfson, D. N., and Dobson, C. M. (1991) *Proteins* **9,** 248–266
55. Encinar, J. A., Fernandez, A. M., Molina, M. L., Molina, A., Poveda, J. A., Albar, J. P., Lopez-Barneo, J., Gavilanes, F., Ferrer-Montiel, A. V., and Gonzalez-Ros, J. M. (2002) *Biochemistry* **41,** 12263–12269
56. Carlomagno, T. (2005) *Annu. Rev. Biophys. Biomol. Struct.* **34,** 245–266
57. Post, C. B. (2003) *Curr. Opin. Struct. Biol.* **13,** 581–588